

*Passive Structures*, T. Itoh, Ed. New York: Wiley, 1989, ch. 7, pp. 447–495.

[24] A. Taflove, “Review of the formulation and applications of the finite-difference time-domain method for numerical modeling of electromagnetic wave interactions with arbitrary structures,” *Wave Motion*, vol. 10, no. 6, pp. 547–582, 1988.

[25] Z. P. Liao, H. L. Wong, B.-P. Yang, and Y.-F. Yuan, “A transmitting boundary for transient wave analysis,” *Sci. Sin., Ser. A*, vol. 27, no. 10, pp. 1063–1076, 1984.

[26] C. E. Reuter, R. M. Joseph, E. T. Thiele, D. S. Katz, and A. Taflove, “Ultrawideband absorbing boundary condition for termination of waveguiding structures in FDTD simulations,” *IEEE Microwave Guided Wave Lett.*, vol. 4, no. 10, pp. 344–346, 1994.

[27] X. P. Lin and K. Naishadham, “A simple technique for the minimization of ABC-induced error in the FDTD analysis of microstrip discontinuities,” *IEEE Microwave Guided Wave Lett.*, vol. 4, no. 12, pp. 402–404, 1994.

[28] F. Giannini, G. Bartolucci and M. Ruggieri, “Equivalent circuit models for computer aided design of microstrip rectangular structures,” *IEEE Trans. Microwave Theory Tech.*, vol. 40, no. 2, pp. 378–388, 1992.

### Scattering by a Thick Off-Centered Circular Iris in Circular Waveguide

Zhongxiang Shen and Robert H. MacPhie

**Abstract**—A formally exact solution is described for the problems of scattering at a junction between two circular waveguides with their axes offset and at a thick off-centered iris in circular waveguide. The analysis method uses Graf’s addition theorem for cylindrical functions and the conservation of complex power technique (CCPT). Sample numerical results are presented and compared with available data in the literature.

### I. INTRODUCTION

Waveguide iris coupling has found many applications in microwave engineering. Circular irises can be used as matching elements in microwave circuits or in waveguide filters. The problem of a circular iris in circular waveguide or the related step junction of two circular waveguides has been considered by many authors. Marcuvitz [1] gave the equivalent shunt susceptance for the  $TE_{11}$  mode excitation of small apertures. English [2] studied the mode conversion at a symmetric step-discontinuity in circular waveguide. Scharstein and Adams [3], [4] treated the problems of a  $TE_{11}$  mode circular waveguide with thin and thick circular irises. Carin *et al.* [5] investigated dielectric matched windows in circular waveguide. Most of the previously published works, however, have been limited to circular irises concentric with the axis of the circular waveguide. Although a simple expression of the equivalent shunt susceptance is available in [1] for the off-centered iris in circular waveguide, the expression is roughly approximate, and limited to the case of small aperture and of zero-thickness.

This paper gives a formally exact solution for the problem of a thick off-centered circular iris in circular waveguide. The conservation of complex power technique (CCPT), which has been used to obtain theoretically exact solutions with numerically convergent results to

Manuscript received December 19, 1994; revised August 1, 1995.

The authors are with the Department of Electrical and Computer Engineering, University of Waterloo, Waterloo, Ontario, Canada N2L 3GL. This work was supported by the Natural Sciences and Engineering Research Council (NSERC) of Canada Grant A-2176.

IEEE Log Number 9414841.

the problem of scattering at certain waveguide junctions [6], [7], and [8], and Graf’s addition theorem for Bessel functions [9] are employed to obtain an analytical solution for the scattering matrix of a junction between two circular waveguides with their axes offset. The generalized scattering matrix technique [10] is then applied to deduce the scattering parameters of the off-centered iris in circular waveguide. Numerical results are presented and compared with those obtained by the approximate formula given in the *Waveguide Handbook* [1].

### II. FORMULATION

Fig. 1 shows the structure of a circular waveguide of radius  $a_2$  loaded with an off-centered circular iris of radius  $a_1$ .  $(d, \theta)$  are the polar coordinates of the center of the small circular waveguide in the coordinate system with its origin at the center of the larger waveguide (as illustrated in Fig. 1). Since the CCPT was well documented in [6], [7], and [8], only a summary of the formulation will be given here. The four scattering submatrices of the junction between guides 1 and 2 shown in Fig. 1 have the following form

$$S_{11} = (\mathbf{Y}_1 + \mathbf{M}^T \mathbf{Y}_2 \mathbf{M})^{-1} (\mathbf{Y}_1 - \mathbf{M}^T \mathbf{Y}_2 \mathbf{M}) \quad (1)$$

$$S_{21} = \mathbf{M} (S_{11} + \mathbf{I}) \quad (2)$$

$$S_{12} = \mathbf{Y}_1^{-1} S_{21}^T \mathbf{Y}_2 \quad (3)$$

$$S_{22} = \mathbf{M} S_{12} - \mathbf{I} \quad (4)$$

with  $\mathbf{Y}_i$ , for  $i = 1$  and 2, is the modal admittance matrix for the  $i$ th waveguide [8], the superscript  $T$  denotes the transpose operation, and  $\mathbf{M}$  is the  $E$ -field mode-matching matrix whose  $(nm, ki)$ th element is given by

$$M_{nm, ki} = \int_{S_1} (\vec{e}_{2, nm} \cdot \vec{e}_{1, ki}) ds \quad (5)$$

where  $\vec{e}_{i, nm}$  ( $i = 1, 2$ ) being the normalized transverse component of the  $nm$ th mode electric field of guide  $i$ , which has the form as follows

$$\vec{e}_{i, nm} = \frac{\hat{z} \times \nabla_t \psi_{i, nm}^h}{\nabla_t \psi_{i, nm}^e}, \quad \begin{array}{ll} \text{for TE modes} \\ \text{for TM modes} \end{array} \quad (6)$$

where

$$\psi_{i, nm}^h = N_{nm}^h J_n \left( \frac{\rho_i x'_{nm}}{a_i} \right) \begin{pmatrix} \sin(n\varphi_i) \\ \cos(n\varphi_i) \end{pmatrix} \quad (7)$$

$$\psi_{i, nm}^e = N_{nm}^e J_n \left( \frac{\rho_i x_{nm}}{a_i} \right) \begin{pmatrix} \cos(n\varphi_i) \\ \sin(n\varphi_i) \end{pmatrix} \quad (8)$$

with

$$N_{nm}^h = \sqrt{\frac{\epsilon_n}{\pi}} \frac{1}{\sqrt{(x'_{nm})^2 - n^2} J_n(x'_{nm})} \quad (9)$$

$$N_{nm}^e = \sqrt{\frac{\epsilon_n}{\pi}} \frac{1}{x_{nm} J_{n+1}(x_{nm})} \quad (10)$$

being normalization constants,  $\epsilon_n = 1$  for  $n = 0$ , and 2 for  $n > 0$ , and  $x'_{nm}$  and  $x_{nm}$  are, respectively, the  $m$ th zeros of  $J'_n(x)$  and  $J_n(x)$ .

Since the integration in (5) is over the cross section of the small waveguide  $S_1$ , we must employ a coordinate transformation between

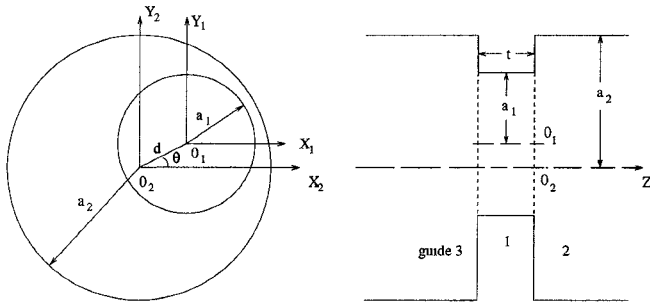
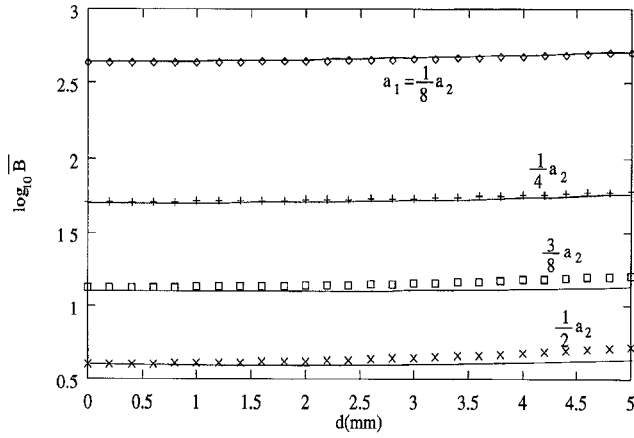


Fig. 1. A thick off-centered circular iris in circular waveguide.

Fig. 2. Normalized shunting susceptance of an off-centered circular iris of zero-thickness in circular waveguide. Line: our results; dots: [1] ( $a_2 = 11.5625$  mm,  $f = 9.375$  GHz,  $t = 0$ ,  $\theta = 0^\circ$ ).

$(\rho_1, \varphi_1)$  and  $(\rho_2, \varphi_2)$  to express  $\vec{e}_{2,nm}$  in terms of  $(\rho_1, \varphi_1)$ . In order to do so, Graf's addition theorem for Bessel functions [9] is used

$$J_n(\lambda\rho_2) \begin{pmatrix} \cos(n\varphi_2) \\ \sin(n\varphi_2) \end{pmatrix} = \sum_{p=-\infty}^{\infty} (-1)^{p+n} J_p(\lambda\rho_1) \cdot J_{p-n}(\lambda d) \begin{pmatrix} \cos[p\varphi_1 - (p-n)\theta] \\ \sin[p\varphi_1 - (p-n)\theta] \end{pmatrix} \quad (11)$$

where  $\lambda$  is an arbitrary constant. Substituting (11) into (7) and (8) we obtain the expression of  $\vec{e}_{2,nm}$  in terms of  $(\rho_1, \varphi_1)$  by using (6). Finally, the elements of the  $E$ -field mode-matching matrix  $\mathbf{M}$  can be derived according to (5), which are elucidated in the Appendix.

After obtaining the scattering matrix of the junction between two offset circular waveguides, we can then treat the problem of an off-centered circular iris of thickness  $t$  in circular waveguide. Fig. 1 illustrates the structure which can be regarded as a cascaded connection of two junctions and the generalized scattering matrix technique [10] may be used to determine the overall scattering matrix  $\mathbf{S}^w$ .

$$\mathbf{S}_{22}^w = \mathbf{S}_{33}^w = \mathbf{S}_{22} + \mathbf{S}_{21} \mathbf{L} \mathbf{S}_{11} (\mathbf{I} - \mathbf{L} \mathbf{S}_{11} \mathbf{L} \mathbf{S}_{11})^{-1} \mathbf{L} \mathbf{S}_{12} \quad (12)$$

$$\mathbf{S}_{23}^w = \mathbf{S}_{32}^w = \mathbf{S}_{21} (\mathbf{I} - \mathbf{L} \mathbf{S}_{11} \mathbf{L} \mathbf{S}_{11})^{-1} \mathbf{L} \mathbf{S}_{12} \quad (13)$$

where  $\mathbf{L}$  is a diagonal transmission matrix of the iris waveguide with

$$L_{k_1, k_2} = \exp(-\gamma_{1, k_1} t) \quad (14)$$

as its  $k_1$ -th diagonal element and the subscript 1 indicates the small iris waveguide.

TABLE I

RELATIVE CONVERGENCE OF THE NORMALIZED SUSCEPTANCE  $\bar{B}$  OF A JUNCTION BETWEEN TWO CIRCULAR WAVEGUIDES WITH THEIR AXES OFFSET ( $d = 2$  mm,  $\theta = 0^\circ$ ,  $a_2 = 11.5626$  mm,  $f = 9.375$  GHz)

$a_1 = a_2/2$			$a_1 = a_2/8$						
$N_1$	$N_2$	$\bar{B}$	$N_1$	$N_2$	$\bar{B}$				
TE	TM	TE	TM	TE	TM				
2	2	4	4	7.782	2	2	128	64	622.29
2	2	8	6	8.154	2	2	192	120	631.93
2	2	18	16	8.223	2	2	320	200	635.19
4	4	8	8	7.719	4	2	128	64	598.87
4	4	18	16	7.856	4	2	416	128	616.87
4	4	32	28	7.892	4	2	720	200	622.55
9	6	36	24	7.766	8	4	392	120	607.31
9	6	60	40	7.812	8	4	792	300	612.99
9	6	120	72	7.826	8	4	1208	504	618.40

### III. NUMERICAL RESULTS

In our numerical computations, only the case of air-filled waveguides is considered, and the incident mode in the larger circular waveguide is assumed to be the dominant  $TE_{11}$  mode.

We begin with the case of a junction between two circular waveguides with their axes offset horizontally ( $\theta = 0^\circ$ ). It is assumed that no propagating modes exists in the smaller waveguide. The normalized load susceptance of the junction has the form of

$$\bar{B} = j \frac{1 - \Gamma_{11}}{1 + \Gamma_{11}} \quad (15)$$

where  $\Gamma_{11}$  is the reflection coefficient of the dominant  $TE_{11}$  mode. Moreover, we assume that the incident  $TE_{11}$  mode in the larger waveguide is sine-type [see (7)] with  $e_{2,11,\rho}(\rho_2, \varphi_2) = -(Y_{11}^h/\rho_2) J_1(\rho_2 x'_{11}/a_2) \cos \varphi_2$ . As in previous work [8], the numbers of modes assumed in each waveguide strongly depend on their relative size. Table I shows the relative convergence of the normalized susceptance  $\bar{B}$  with respect to  $N_1$  and  $N_2$ , where  $N_1$  and  $N_2$  are the numbers of modes retained in the smaller and the larger circular waveguides, respectively. It is seen that when the radius  $a_1$  of the smaller waveguide is very small compared with  $a_2$ , we should take more modes of the larger waveguide into account to obtain convergent results. It is expected that the shift  $d$  between these two axes of the waveguides also has a noticeable effect on the convergence behavior.

To compare our results with those obtained by the approximate formula given in [1], we consider the case of the circular iris with zero thickness. For this case, the effect of the zero-thickness iris may be characterized by a shunting susceptance  $\bar{B} = B/Y_{11}$  normalized with respect to the  $TE_{11}$  mode's characteristic admittance  $Y_{11}$ . Numerical results for the normalized shunting susceptance of a thin ( $t = 0$ ) off-centered iris in circular waveguide are presented in Fig. 2. The results are compared with those calculated by the approximate formula provided by the *Waveguide Handbook* [1]. We note that the agreement between the closed-form approximate solution [1] and our rigorous scattering matrix solution is good for small aperture; but for the case of large aperture the difference between them is significant as is expected.

The effect of the location of a small iris on the normalized shunting susceptance  $\bar{B}$  is shown in Fig. 3. When  $\theta = 90^\circ$  or  $270^\circ$ ,  $\bar{B}$  reaches its maximum.

The magnitudes and phases of the reflection coefficient  $\Gamma_{11}$  and transmission coefficient  $T_{11}$  of the dominant  $TE_{11}$  mode in a circular waveguide loaded with a thick off-centered iris are plotted in Fig. 4 as functions of thickness  $t$ . When the shift  $d$  between two axes

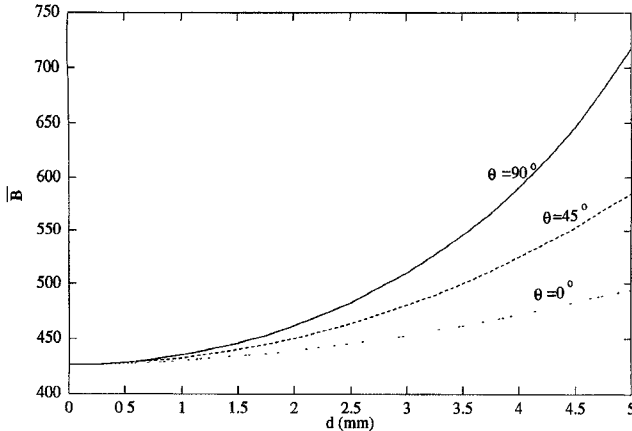


Fig. 3. Normalized shunting susceptance of an off-centered circular iris of zero-thickness in circular waveguide ( $a_2 = 11.5625$  mm,  $f = 9.375$  GHz,  $t = 0$ ,  $a_1 = a_2/8$ ).

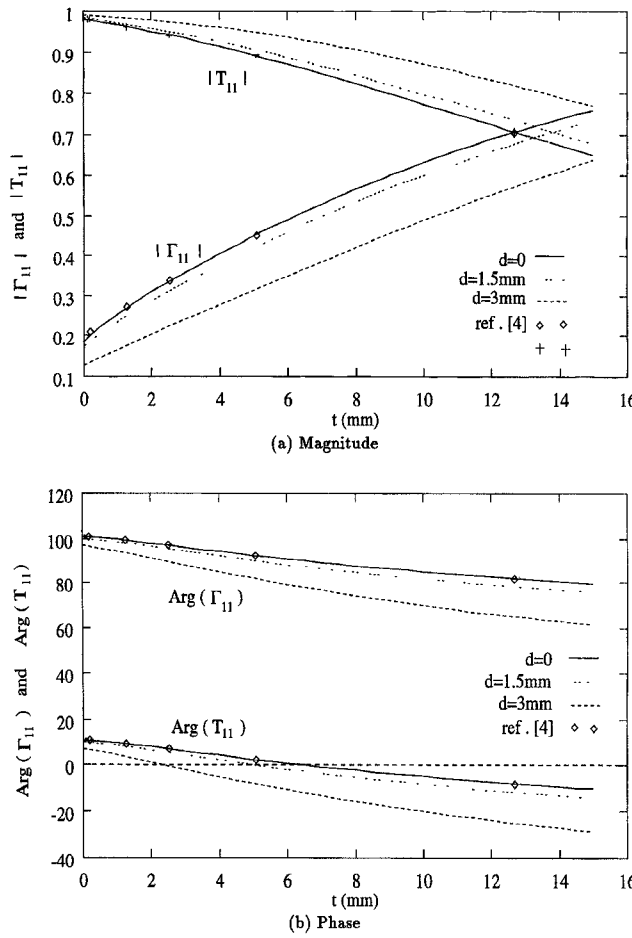


Fig. 4. Magnitudes and phases of the transmission coefficient  $T_{11}$  of a thick iris in circular waveguide for different  $d$ . ( $a_1 = 9.525$  mm,  $a_2 = 12.74445$  mm,  $f = 9$  GHz,  $\theta = 0^\circ$ ).

vanishes, the problem considered reduces to that treated by Scharstein and Adams [4]. For this centered case, it is seen that our results are in good agreement with those in [4]. It is noted that when the thickness of the iris increases, the magnitude of reflection coefficient (transmission coefficient) goes to 1 (0). This is obvious because no modes can propagate in the iris waveguide and less and less energy tunnels across the iris as its thickness increases.

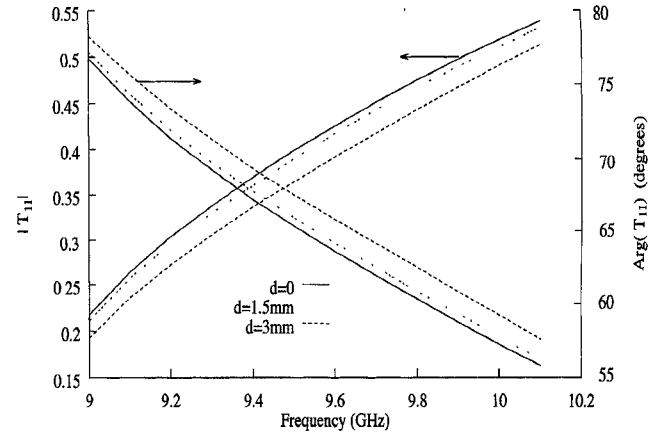


Fig. 5. Magnitude and phase of the transmission coefficient  $T_{11}$  for a thick iris in circular waveguide ( $a_1 = 6$  mm,  $a_2 = 10$  mm,  $t = 0.5$  mm,  $\theta = 0^\circ$ ).

An interesting phenomenon in Fig. 4 is that the transmission coefficient for an off-centered iris is greater than that of a centered iris. This property may be attributed to the fact that for the off-centered case more lower-order modes in the iris waveguide are excited and less attenuated when they reach the other side of the iris. This curious phenomenon also occurs for the offset rectangular iris in rectangular waveguide.

The magnitude and phase of the transmission coefficient  $T_{11}$  are given in Fig. 5 for different values of shift  $d$ . It is seen that when the working frequency increases, the transmission coefficient becomes bigger. That is to say, more power can tunnel across the iris when the frequency increases since the higher-order modes in the smaller waveguide are less attenuated.

#### IV. CONCLUSION

This paper has provided a formally exact modal solution with convergent numerical results to the problem of a thick off-centered circular iris in a circular waveguide. The off-centered iris has more design flexibilities than the centered iris and provides the advantage of a larger susceptance range. Moreover, circular irises (centered or offset) are much easier to manufacture than rectangular irises. The present work may have applications in matched windows in circular waveguide [5], in constructing filters as a block element, and in the coupling to a dual mode circular cavity by a circular hole.

#### APPENDIX

The overall  $E$ -field mode-matching matrix  $M$  has the following form

$$M = \begin{bmatrix} [M_{nm,ki}^{hh}] & [M_{nm,ki}^{he}] \\ [M_{nm,ki}^{eh}] & [M_{nm,ki}^{ee}] \end{bmatrix} \quad (16)$$

where

$$M_{nm,ki}^{hh} = (-1)^k \frac{\pi}{a_1 a_2} N_{ki}^h N_{nm}^h (x'_{ki})^2 x'_{nm} \frac{J_k(x'_{ki}) J'_k \left( \frac{a_1 x'_{nm}}{a_2} \right)}{\left( \frac{x'_{ki}}{a_1} \right)^2 - \left( \frac{x'_{nm}}{a_2} \right)^2} Q_1 \quad (17)$$

$$M_{nm,ki}^{he} = 0 \quad (18)$$

$$M_{nm,ki}^{eh} = (-1)^k k \pi N_{ki}^h N_{nm}^e J_k(x'_{ki}) J'_k \left( \frac{a_1 x_{nm}}{a_2} \right) Q_2 \quad (19)$$

$$M_{nm,ki}^{ee} = (-1)^{k+1} \pi N_{ki}^e N_{nm}^e \left( \frac{x_{nm}}{a_2} \right)^2 \frac{J'_k(x'_{ki}) J_k \left( \frac{a_1 x_{nm}}{a_2} \right)}{\left( \frac{x'_{ki}}{a_1} \right)^2 - \left( \frac{x_{nm}}{a_2} \right)^2} Q_3 \quad (20)$$

with

$$Q_1 = J_{k+n} \left( \frac{x'_{nm} d}{a_2} \right) C_1(k+n) + (-1)^n J_{k-n} \left( \frac{x'_{nm} d}{a_2} \right) C_2(k-n) \quad (21)$$

$$Q_2 = -J_{k+n} \left( \frac{x_{nm} d}{a_2} \right) C_2(k+n) + (-1)^n J_{k-n} \left( \frac{x_{nm} d}{a_2} \right) C_1(k-n) \quad (22)$$

$$Q_3 = J_{k+n} \left( \frac{x_{nm} d}{a_2} \right) C_3(k+n) + (-1)^n J_{k-n} \left( \frac{x_{nm} d}{a_2} \right) C_4(k-n) \quad (23)$$

$$C_1(k+n) = \begin{bmatrix} -(\epsilon_k - 1) \cos((k+n)\theta) & \sin((k+n)\theta) \\ (\epsilon_k - 1) \sin((k+n)\theta) & \cos((k+n)\theta) \end{bmatrix} \quad (24)$$

$$C_2(k-n) = \begin{bmatrix} (\epsilon_k - 1) \cos((k-n)\theta) & -\sin((k-n)\theta) \\ (\epsilon_k - 1) \sin((k-n)\theta) & \cos((k-n)\theta) \end{bmatrix} \quad (25)$$

$$C_3(k+n) = \begin{bmatrix} \cos((k+n)\theta) & (\epsilon_k - 1) \sin((k+n)\theta) \\ \sin((k+n)\theta) & -(\epsilon_k - 1) \cos((k+n)\theta) \end{bmatrix} \quad (26)$$

$$C_4(k-n) = \begin{bmatrix} \cos((k-n)\theta) & (\epsilon_k - 1) \sin((k-n)\theta) \\ -\sin((k-n)\theta) & (\epsilon_k - 1) \cos((k-n)\theta) \end{bmatrix} \quad (27)$$

and  $\epsilon_k = 1$  for  $k = 0$ , and 2 for  $k > 0$ .

## REFERENCES

- [1] N. Marcuvitz, *Waveguide Handbook*. New York: McGraw-Hill, 1951.
- [2] W. J. English, "The circular waveguide step-discontinuity transducer," *IEEE Trans. Microwave Theory Tech.*, vol. MTT-21, pp. 633-636, Oct. 1973.
- [3] R. W. Scharstein and A. T. Adams, "Galerkin solution for the thin circular iris in a  $TE_{11}$ -mode circular waveguide," *IEEE Trans. Microwave Theory Tech.*, vol. 36, pp. 106-113, Jan. 1988.
- [4] —, "Thick circular iris in a  $TE_{11}$  circular waveguide," *IEEE Trans. Microwave Theory Tech.*, vol. 36, pp. 1529-1531, Nov. 1988.
- [5] L. Carin, K. J. Webb, and S. Weinreb, "Matched windows in circular waveguide," *IEEE Trans. Microwave Theory Tech.*, vol. 36, pp. 1359-1362, Sept. 1988.
- [6] R. Safavi-Naini and R. H. MacPhie, "Scattering at rectangular-to-rectangular waveguide junctions," *IEEE Trans. Microwave Theory Tech.*, vol. MTT-30, pp. 2060-2063, Nov. 1982.
- [7] R. R. Mansour and R. H. MacPhie, "Scattering at an N-furcated parallel-plate waveguide junction," *IEEE Trans. Microwave Theory Tech.*, vol. MTT-33, pp. 830-835, Sept. 1985.
- [8] J. D. Wade and R. H. MacPhie, "Scattering at circular-to-rectangular waveguide junctions," *IEEE Trans. Microwave Theory Tech.*, vol. MTT-34, pp. 1085-1091, Nov. 1986.
- [9] M. Abramowitz and I. A. Stegun, *Handbook of Mathematical Functions*. New York: Dover, 1965.
- [10] R. Mittra and S. W. Lee, *Analytical Techniques in the Theory of Guided Waves*. New York: Macmillan, 1971.

## Modellization of Losses in $TE_{011}$ -Mode Waveguide Bandpass Filters

Andrea Melloni and G. Guido Gentili

**Abstract**—A mode-matching technique for the analysis of  $TE_{011}$  mode waveguide cylindrical bandpass filters including losses is presented. The modes of a lossy radial waveguide are derived and the generalized scattering matrix of the lossy cavity coupled by two rectangular apertures is computed enforcing an impedance boundary condition on the cavity sidewall. Cavity sidewall losses as well as top and bottom wall losses are therefore taken accurately into account. Numerical and experimental results are given for a four cavity filter in  $K_a$  band.

## I. INTRODUCTION

Cylindrical cavities resonating in  $TE_{011}$ -mode are very attractive for the realization of low-loss narrow-band filters. Fig. 1 shows the structure of a filter section: cylindrical cavities are coupled together and to the external waveguide by means of short rectangular coupling irises operating below cutoff. The two apertures on the cavity sidewall form an angle  $2\theta$ .

In [1], [2] the authors presented a mode-matching technique to analyse accurately this kind of filters. That procedure allowed to take accurately into account the effects of the thick coupling apertures, the irises angular offset  $2\theta$ , the spurious responses and the higher mode interaction between adjacent resonators, overcoming the limitations of available approximate models [3], [4]. After that, by optimization procedures it is possible to design filters having the desired frequency response without resorting to empirical adjustments.

In the present paper, it is explained how to modify this mode matching technique to take into account also ohmic losses. Top, bottom, and cavity sidewall are assumed to have finite conductivity while coupling irises, which are very short and operate below the cutoff, are assumed lossless. Moreover, since in the passband the field configuration inside the cavity is very similar to the  $TE_{011}$  mode only, losses due to currents flowing in the  $x$ -direction, which are due only to spurious modes, are neglected.

For sake of simplicity in this paper the analysis is limited to cavities with two identical apertures symmetrically placed with respect to the height of the cavity. The general case of cavities with two different apertures can be derived with minor modifications of the algorithm.

Sections II and III reports the formal solution of the field problem and Section IV some numerical and experimental results.

## II. STATEMENT OF THE PROBLEM

The analysis of  $TE_{011}$  bandpass filters is conveniently carried out by splitting the whole structure in simpler building blocks, as shown in Fig. 1. Two discontinuities must be analyzed: the symmetrical double-step formed by the junction between the rectangular external waveguide and the first (last) rectangular coupling iris and the discontinuity at the junction between the irises and the cavity itself. Each discontinuity is considered separately and its generalized scattering matrix is computed. The overall scattering matrix of the total filter is hence obtained by a suitable direct combination of all single scattering matrices [5]. The analysis of the double-step discontinuity in rectangular waveguide is a well known problem, efficiently solved

Manuscript received January 6, 1995; revised August 1, 1995.

A. Melloni is with the Politecnico di Milano, Dipartimento di Elettronica e Informazione, I-20133 Milano, Italy.

G. G. Gentili is with CSTS-CNR, Politecnico di Milano, Italy.  
IEEE Log Number 9414847.